

IDENTIFICATION OF GENETIC FACTORS ASSOCIATED WITH CORPUS CALLOSUM MORPHOLOGY: CONDITIONAL STRONG INDEPENDENCE SCREENING FOR NON-EUCLIDEAN RESPONSES

BY ZHE GAO^{1,a}, JIN ZHU^{2,c}, YUE HU^{3,d}, WENLIANG PAN^{4,e} AND XUEQIN WANG^{1,b}

¹*School of Management, University of Science and Technology of China, ^agaozh8@mail.ustc.edu.cn; ^bwangxq20@ustc.edu.cn*

²*Department of Statistics, London School of Economics and Political Science, ^cJ.Zhu69@lse.ac.uk*

³*Yale University School of Public Health ^dyue.hu@yale.edu*

⁴*Academy of Mathematics and Systems Science, Chinese Academy of Sciences ^epanwliang@amss.ac.cn*

The corpus callosum, the largest white matter structure in the brain, plays a critical role in interhemispheric communication. Variations in its morphology are associated with various neurological and psychological conditions, making it a key focus in neurogenetics. Age is known to influence the structure and morphology of the corpus callosum significantly, complicating the identification of specific genetic factors that contribute to its shape and size. We propose a conditional strong independence screening method to address these challenges for ultrahigh-dimensional predictors and non-Euclidean responses. Our approach incorporates prior knowledge, such as age. It introduces a novel concept of conditional metric dependence, quantifying non-linear conditional dependencies among random objects in metric spaces without relying on predefined models. We apply this framework to identify genetic factors associated with the morphology of the corpus callosum. Simulation results demonstrate the efficacy of this method across various non-Euclidean data types, highlighting its potential to drive genetic discovery in neuroscience.

1. Introduction. Neuroscience has seen transformative advancements, moving from basic anatomical studies to highly sophisticated computational analyses. The advent of neuroimaging technologies, such as magnetic resonance imaging (MRI), diffusion tensor imaging (DTI), and positron emission tomography (PET), has revolutionized the way we visualize and understand the brain's complex structures. These innovations have deepened our insights into neural anatomy and function while introducing non-Euclidean data that require novel analytical methods. One prominent example is the corpus callosum, the brain's largest white matter structure. Comprising approximately 200 million myelinated nerve fibers, it is the primary connection between the left and right hemispheres (Tanaka-Arakawa et al., 2015). These fibers form homotopic and heterotopic projections, enabling the integration and transfer of sensory, motor, and cognitive information between hemispheres (Kennedy, Van Essen and Christen, 2016). Changes in the size and shape of the corpus callosum can significantly impact its function and have been associated with several neurological conditions, including Alzheimer's disease (Bachman et al., 2014), schizophrenia, and bipolar disorder (Vermeulen et al., 2023).

The goal of genome-wide association studies (GWAS) that look into brain structure is to find out how genetic factors affect the structure and function of the brain. Researchers often collect high-dimensional genetic data and neurological metrics to do this. Along with genetic information, covariates like age and disease status are often included because they

Keywords and phrases: Conditional metric dependence, Conditional strong independence screening, Non-Euclidean response, Ultrahigh-dimensional data analysis.

significantly affect brain structure (Cornea et al., 2016; Biswal et al., 2010). However, the specific genetic factors that shape the morphology of the corpus callosum remain largely unexplored. Given the critical role of covariates like age in influencing corpus callosum structure, assessing the conditional contributions of genetic factors while adjusting for these covariates to identify key genetic determinants is essential. Identifying relevant factors from high-dimensional data while accounting for essential covariates remains crucial in analyzing non-Euclidean data.

To address the challenge of high-dimensional data analysis, Barut, Fan and Verhasselt (2016) introduced conditional sure independence screening (CSIS) within the generalized linear model framework, expanding upon the original sure independence screening (SIS) method (Fan and Lv, 2008). CSIS evaluates the conditional maximum likelihood estimator to measure marginal utility and selects variables with high marginal utility. Since its inception, CSIS has been adapted to various contexts. For instance, Hu and Lin (2017) developed an empirical-likelihood-based CSIS for less restrictive distributional assumptions, while Hong, Kang and Li (2018) introduced a version for censored responses. Furthermore, Chen et al. (2019) suggested a model-free version, and Wen et al. (2018) made a conditional distance correlation-based CSIS for responses with multiple variables. CSIS has also been extended to survival data Lu, Chen and Wang (2019). Other changes include an adaptive CSIS created by Lin and Sun (2016) to cut down on false positives and negatives, as well as robust CSIS methods for weaker model assumptions created by Hong, Wang and He (2016) and Zhang, Pan and Zhou (2018). Furthermore, Liu and Chen (2018) suggested a conditional quantile independence screening method to find features that affect the conditional quantiles of the response without defining a model structure, and Zheng, Hong and Li (2020) introduced a sequential conditioning method that updates the conditioning set over and over again.

Despite these numerous extensions, none of the existing CSIS methods are designed explicitly for non-Euclidean responses. This gap underscores the need for new approaches to handle the complex data structures encountered in modern neurogenetic studies.

This article aims to explore genetic factors influencing the shape of the corpus callosum by introducing a novel conditional screening method that addresses these gaps. Methodologically, we propose a model-free and distribution-free procedure called Conditional Metric Dependence-based Conditional Strong Independence Screening (COME-CSIS). Theoretically, COME-CSIS has been proven effective across a wide range of non-Euclidean data and exhibits strong screening properties in ultra-high-dimensional settings. In addition, COME-CSIS offers several significant advantages. It is robust, allowing for less restrictive moment conditions on both explanatory variables and the response. Its corresponding marginal utility enables conditional dependence analysis in non-Euclidean spaces, which has remained largely unexplored.

By applying COME-CSIS to both synthetic and real datasets, we demonstrate its ability to overcome the limitations of the strong negative type (Lyons, 2013), establishing it as a valuable tool for ultrahigh-dimensional non-Euclidean data analysis. In the real-data application, COME-CSIS was employed to identify genes associated with the shape of the corpus callosum. Compared to existing screening methods, our approach avoided selecting genes related primarily to age or Alzheimer’s disease, which are well-known factors influencing corpus callosum morphology. These results provide important preliminary insights into the gene regulation mechanisms affecting the corpus callosum and open the door for further investigation.

The following contents are organized as follows: In Section 2, we introduce notation and formulate our problem. Then, we propose a novel marginal utility for CSIS and a related CSIS procedure and study their theoretical properties in Section 3. In Section 4, we analyze a real-world dataset to demonstrate the helpfulness of our method. In Section 5, we

conduct simulation studies to evaluate the performance of our method. Finally, we conclude this article with a few remarks in Section 6. All of the technical details are deferred to the supplementary materials.

2. Preliminaries. The section will introduce notations and formulate our problem in subsection 2.1 and 2.2, respectively.

2.1. Notations. Suppose $(\mathcal{X}, d_{\mathcal{X}})$ is a separable metric space. For any $x_1, x_2 \in \mathcal{X}$, the closed ball with the center x_1 and the radius $d_{\mathcal{X}}(x_1, x_2)$ is denoted as $\bar{B}_{\mathcal{X}}(x_1, x_2)$. Let $(\mathcal{Y}, d_{\mathcal{Y}})$ be another separable metric space and $d_{\mathcal{X} \times \mathcal{Y}}((x_1, y_1), (x_2, y_2)) = \|(d_{\mathcal{X}}(x_1, x_2), d_{\mathcal{Y}}(y_1, y_2))\|_2^2$, we define their product metric space as $(\mathcal{X} \times \mathcal{Y}, d_{\mathcal{X} \times \mathcal{Y}})$. Next, we define the project operator in metric spaces: $\pi_{\mathcal{X}}(\cdot) : \mathcal{X} \times \mathcal{Y} \rightarrow \mathcal{X}$ is the projection on \mathcal{X} satisfying $\pi_{\mathcal{X}}((x, y)) = x$, where $(x, y) \in \mathcal{X} \times \mathcal{Y}$. For a set $\mathcal{K} \subset \mathcal{X} \times \mathcal{Y}$, $\pi_{\mathcal{X}}(\mathcal{K}) = \bigcup_{(x,y) \in \mathcal{K}} \{x\}$. The definition of $\pi_{\mathcal{Y}}(\mathcal{K})$ is the same.

Let (X_1, \dots, X_p, Y, Z) be a random variable defined on a probability space, where Y is a metric-valued variable, and X_1, \dots, X_p, Z are Euclidean-valued variables with dimensionality d_1, \dots, d_p, d_z . Suppose $\sigma(Z)$ is complete such that the regular conditional probabilities of $(X_1, Y), \dots, (X_p, Y), (X_1, \dots, X_p, Y)$ given Z are existing. Let $\{(X_{1i}, \dots, X_{pi}, Y_i, Z_i)\}_{i=1}^n$ be an *i.i.d.* sample of (X_1, \dots, X_p, Y, Z) . Suppose $I(\cdot)$ is an indicator function, we define $\delta_{ij,k}^{X_r} = I(X_{rk} \in \bar{B}_{\mathbb{R}^{d_r}}(X_{ri}, X_{rj}))$, which indicates whether X_{rk} is located in $\bar{B}_{\mathbb{R}^{d_r}}(X_{ri}, X_{rj})$, and $\delta_{ij,kl}^{X_r} = \delta_{ij,k}^{X_r} \delta_{ij,l}^{X_r}$, which is an indicator for whether both of X_{rk} and X_{rl} fall into $\bar{B}_{\mathbb{R}^{d_r}}(X_{ri}, X_{rj})$. Also, let $\eta_{ij,klst}^{X_r} = (\delta_{ij,kl}^{X_r} + \delta_{ij,st}^{X_r} - \delta_{ij,ks}^{X_r} - \delta_{ij,lt}^{X_r})/2$. Analogously, define the notations $\delta_{ij,k}^Y, \delta_{ij,kl}^Y$ and $\eta_{ij,klst}^Y$ for Y .

2.2. Problem formulation. We precisely formulate the problem in the article as follows. We are interested in developing a procedure to exclude the following variables:

$$\mathcal{I} = \{r \mid r \in \{1, \dots, p\} \text{ and } X_r \perp\!\!\!\perp Y \mid Z\}$$

but retain:

$$\mathcal{A} = \{r \mid r \in \{1, \dots, p\} \text{ and } X_r \not\perp\!\!\!\perp Y \mid Z\},$$

where $\perp\!\!\!\perp$ and $\not\perp\!\!\!\perp$ mean conditional independence and dependence, respectively.

3. Methods.

3.1. Conditional metric dependence (COME). We will present two types of conditional metric dependence (COME): conditional ball covariance and global conditional ball correlation in this part. Denote the regular conditional probabilities of $(X, Y), X, Y$ given Z as $\mu_{XY|Z}, \mu_{X|Z}, \mu_{Y|Z}$. Here, for notation convenience, we have suppressed notational dependence on r and assumed X is a d -dimensional; thus, the following content holds for each $r \in \{1, \dots, p\}$ and $d \in \mathbb{N}^+$. Our key idea for the COME measures is to evaluate the difference between $\mu_{XY|Z}$ and the product measure of $\mu_{X|Z}$ and $\mu_{Y|Z}$ on the ball. We first present the definitions of conditional ball covariance.

DEFINITION 1. The conditional ball covariance is defined as

$$\begin{aligned} \mathcal{V}^2(X, Y|Z) = & \int \left[\mu_{XY|Z}(\bar{B}_{\mathbb{R}^d}(x_1, x_2) \times \bar{B}_{\mathcal{Y}}(y_1, y_2)) - \mu_{X|Z}(\bar{B}_{\mathbb{R}^d}(x_1, x_2)) \mu_{Y|Z}(\bar{B}_{\mathcal{Y}}(y_1, y_2)) \right]^2 \\ & \times \mu_{XY|Z}(dx_1, dy_1) \mu_{XY|Z}(dx_2, dy_2). \end{aligned}$$

Notably, $\mathcal{V}^2(X, Y|Z)$ is a non-negative random variables of Z . It evaluates the conditional dependence between X and Y for all points in the support set of Z , and thus, it can be considered as a ‘‘local’’ conditional dependence measure. Next, we present a ‘‘global’’ measure for conditional dependence.

DEFINITION 2. The global conditional ball correlation is

$$\tau = E[\mathcal{R}^2(X, Y|Z)],$$

where $\mathcal{R}^2(X, Y|Z) = \frac{\mathcal{V}^2(X, Y|Z)}{\sqrt{\mathcal{V}^2(X, X|Z)\mathcal{V}^2(Y, Y|Z)}}$ if $\mathcal{V}^2(X, X|Z)\mathcal{V}^2(Y, Y|Z) > 0$, and 0 otherwise.

Next, we show that the two COME measures are proper conditional dependence measures under mild conditions. Our first condition is related to probability measures. Let \mathbf{M}_1 be a collection of discrete Borel probability measures on $\mathbb{R}^d \times \mathcal{Y}$, and \mathbf{M}_2 be a collection of Borel probability measures on $\mathbb{R}^d \times \mathcal{Y}$ such that $\forall (x_1, y_1) \in \mathbb{R}^d \times \mathcal{Y}$ and $(x_2, y_2) \sim \mu_{XY|Z}$, $(d_{\mathbb{R}^d}(x_1, x_2), d_{\mathcal{Y}}(y_1, y_2))$ has a continuous density function. The first condition is:

(C1) Both $\mu_{X|Z}$ and $\mu_{Y|Z}$ are convex combinations of elements in \mathbf{M}_1 and \mathbf{M}_2 .

The second assumption is about a geometrical property of separable metric space $(\mathcal{Y}, d_{\mathcal{Y}})$, called directionally (ϵ, ξ, L) -limited (Federer, 2014). The metric $d_{\mathcal{Y}}$ is called directionally (ϵ, ξ, L) -limited at the subset S of \mathcal{Y} , if for $S \subseteq \mathcal{Y}$, there exist $\epsilon > 0$, $\xi \in (0, 1/3]$, $L \in \mathbb{N}^+$, and the following statement holds: if for each $a \in S$, $D \subseteq S \cap \bar{B}_{\mathcal{Y}}(a, \epsilon)$ such that $d(y, c) \geq \xi d(a, c)$ whenever $b, c \in D$ ($b \neq c$), $d(a, b) \geq d(a, c)$, $y \in \mathcal{Y}$ with $d(a, y) = d(a, c)$, $d(y, b) = d(a, b) - d(a, y)$, then the cardinality of D is no larger than L . Our second condition relies on this property:

(C2) For a series of compact set $\mathcal{K} \subseteq \mathbb{R}^d \times \mathcal{Y}$ such that $\mu(\mathcal{K}) \geq 1 - \epsilon$ (or $\nu(\mathcal{K}) \geq 1 - \epsilon$) for every $\epsilon > 0$, $d_{\mathcal{Y}}$ is directionally $(\epsilon(\pi_{\mathcal{Y}}(\mathcal{K})), \eta(\pi_{\mathcal{Y}}(\mathcal{K})), L(\pi_{\mathcal{Y}}(\mathcal{K})))$ -limited at $\pi_{\mathcal{Y}}(\mathcal{K})$.

The theorem below guarantees the COME measures are proper measurements for conditional dependence.

THEOREM 1. If (C1) and (C2) hold, the following properties hold:

- (i) $\mathcal{V}^2(X, Y|Z) \geq 0$ almost surely, and the equality holds if and only if $X \perp\!\!\!\perp Y|Z$.
- (ii) $0 \leq \tau \leq 1$, and $\tau = 0$ if and only if $X \perp\!\!\!\perp Y|Z$.

Theorem 1 shows that, under mild conditions, $\mathcal{V}^2(X, Y|Z) \stackrel{a.s.}{=} 0$ and $\tau = 0$ are equivalent to conditional independence. Many well-known conditional independence measures satisfy similar conditional-independence equivalence, like the kernel conditional dependence measures (Fukumizu et al., 2008) and the conditional distance correlation (Wang et al., 2015). Many metric spaces encountered in non-Euclidean data analysis are directionally limited, such as Riemannian manifolds and Phylogenetic tree spaces (Wang et al., 2021).

For practical usage, we propose the COME estimators. We first show that the conditional ball covariance is the conditional expectation of two random variables:

THEOREM 2. A variable-separated variant of the conditional ball covariance is given as follows,

$$\mathcal{V}^2(X, Y|Z = z) = E\{\eta_{12,3456}^X \eta_{12,3456}^Y | Z_1, \dots, Z_6 = z\}.$$

Let $\mathcal{W}^{X,Y}(z) = E\{\eta_{12,3456}^X \eta_{12,3456}^Y | Z_1, \dots, Z_6 = z\}$, Theorem 2 implies $\mathcal{R}^2(X, Y | Z = z) = \mathcal{W}^{X,Y}(z) / \sqrt{\mathcal{W}^{X,X}(z) \mathcal{W}^{Y,Y}(z)}$ if $\mathcal{W}^{X,X}(z) \mathcal{W}^{Y,Y}(z) > 0$ and 0 otherwise. Theorem 2 motivates us to estimate τ with V-processes and density estimation of Z . Denote H and $K(\cdot)$ as bandwidth matrix and kernel function, respectively. Let $\hat{f}_k(z) = (n|H|)^{-1} K(H^{-1}(z - Z_k))$, the kernel density estimation for $Z = z$ is presented as $\hat{f}(z) = \sum_{k=1}^n \hat{f}_k(z)$. Then $\mathcal{W}^{X,Y}(z)$ can be estimated by the empirical V-process:

$$\mathcal{W}_n^{XY}(z) = \sum_{i,j,k,l,s,t=1}^n \frac{\hat{f}_i(z) \hat{f}_j(z) \hat{f}_k(z) \hat{f}_l(z) \hat{f}_s(z) \hat{f}_t(z)}{\hat{f}^6(z)} \eta_{ijklst}^X \eta_{ijklst}^Y.$$

And $\mathcal{R}^2(X, Y | Z = z)$ can be estimated by:

$$\mathcal{R}_n^2(X, Y | Z = z) = \mathcal{W}_n^{XY}(z) / \sqrt{\mathcal{W}_n^{XX}(z) \mathcal{W}_n^{YY}(z)},$$

if $\mathcal{W}_n^{XX}(z) \mathcal{W}_n^{YY}(z) > 0$, and 0 otherwise. From the definition of τ , it can be estimated by

$$(1) \quad \hat{\tau} = \frac{1}{n} \sum_{u=1}^n \mathcal{R}_n^2(X, Y | Z = z_u).$$

The computation burden would be extremely heavy if computing $\hat{\tau}$ according to its exact definition (1). In supplementary material, we will develop a method to significantly reduce the time complexity of computing $\hat{\tau}$.

3.2. COME based conditional strong independence screening. The section establishes a novel CSIS procedure to tackle the problem formulated in subsection 2.2. According to Theorem 1, under mild conditions, the global ball condition correlation equal to zero is equivalent to the conditional independence thereby, we have:

$$\mathcal{A} = \{r \mid \tau_r > 0\} \text{ and } \mathcal{I} = \{r \mid \tau_r = 0\},$$

where τ_r is the global conditional ball correlation between X_r and Y given Z . This fact motivates us to calculate the global conditional ball correlation for pair (X_r, Y, Z) as a marginal utility to assess the influence of X_r on the response Y given Z , and then filter out the variables with zero global conditional metric dependence. Based on this motivation, we propose a two-step procedure, COME-based conditional strong independence screening (COME-CSIS):

- (i) Given a dataset $\{(X_{1i}, \dots, X_{pi}, Y_i, Z_i)\}_{i=1}^n$, we compute $\hat{\tau}_1, \dots, \hat{\tau}_p$ according to (1);
- (ii) Using $\hat{\tau}_i$ as a marginal utility, we pick out the d_n most important variables, i.e.,

$$\mathcal{M}_{d_n} = \{r \mid \hat{\tau}_r \text{ is the first } d_n \text{ largest of } \{\hat{\tau}_1, \dots, \hat{\tau}_p\}\}.$$

Note that, in step (i), $\hat{\tau}_r$ serves as a surrogate of τ_r since τ_r is unknown in reality and needs to be estimated by data; and in step (ii), d_n is related to n (Fan and Lv, 2008).

Next, we study the strong screening property of the COME-CSIS, which ensures that $\mathcal{M}_{d_n} = \mathcal{A}$ with high probability. The strong screening property asserts a more desirable result than the sure screening property, which only guarantees $\mathcal{A} \subseteq \mathcal{M}_{d_n}$. Such a property is also for recently advanced screening methods such as Huang, Li and Wang (2014) and Pan et al. (2019). As an illustration, we apply the COME-CSIS to synthetic datasets detailed in Section 5.1, and the probability of $\mathcal{M}_{d_n} = \mathcal{A}$ is shown in Figure 1. From Figure 1, the probability that our proposal exactly identifies \mathcal{A} increases to one as the sample size increases.

To derive the strong screening of the COME-CSIS, we impose some conditions as follows.

- (C3) The kernel function $K(\cdot)$ is non-negative and uniformly-bounded, and the bandwidth for kernel estimation of Z satisfies $h = O(n^{-\kappa/(2d_z)})$, where $0 \leq \kappa < 1/2$.

(C4) If Z_1, \dots, Z_6 are independent copies of Z , then for $1 \leq r \leq p$, there exists a positive constant L , such that

$$\max_r |E(\zeta_{123456,r} | Z_1, Z_2, Z_3, Z_4, Z_5, Z_6) - E(\zeta_{123456,r} | Z'_1, Z_2, Z_3, Z_4, Z_5, Z_6)| \leq L \|Z_1 - Z'_1\|.$$

(C5) There exists a positive constant s_0 such that for all $0 < s \leq s_0$ and $z \in \text{supp}\{Z\}$,

$$E[\exp(sK_H(Z - z) \|Z - z\|)] < \infty.$$

(C6) There exist some constants $c > 0$ and $0 \leq \kappa < 1/2$ such that

$$\min_{r \in \mathcal{A}} \tau_r \geq 2cn^{-\kappa}.$$

Condition (C3) imposes a mild condition on the kernel function, and most existing kernel functions satisfy this regularity condition. It also claims that the bandwidth of kernel estimation of Z satisfies $h = O(n^{-\kappa/(2d_z)})$. This requirement for bandwidth helps guarantee the density estimate is consistent. The works of [Liu, Li and Wu \(2014\)](#) and [Wen et al. \(2018\)](#) also rely on similar conditions. To make Condition (C3) hold, the kernel function is set as a rectangle kernel, and its bandwidth is set as $h = n^{-1/(6d_z)}$ in our implementation. Condition (C4) is satisfied if the first order partial derivative of $E(\zeta_{123456,r} | Z_1, Z_2, Z_3, Z_4, Z_5, Z_6)$ are all bounded, which is similar to one of condition in [Wen et al. \(2018\)](#). Condition (C5) provides an exponential bound on the product of kernel function and the distance of variable Z . Condition (C6) assumes that the minimum true signal has a lower bound with the order of $n^{-\kappa}$, which still allows the minimum true signal to approach zero when the sample size n increases infinity. Assumptions analogous to Condition (C6) are common in the high-dimensional data analysis literature (e.g., [Meinshausen and Buhlmann \(2006\)](#), [Fan and Lv \(2008\)](#), [Barut, Fan and Verhasselt \(2016\)](#), [Xue and Liang \(2017\)](#)). Under these conditions, the following theorem presents the strong screening property of the COME-CSIS:

THEOREM 3 (Strong screening property of the COME-CSIS). *If both the conditions in Theorem 1 and Conditions (C3)-(C5) hold, then for any $0 < \gamma < 1/2 - \kappa$, there exists positive constants c_1 and c_2 such that*

$$\mathbb{P}(\max_{1 \leq r \leq p} |\hat{\tau}_r - \tau_r| \geq cn^{-\kappa}) \leq p[\exp(-c_1 n^{1-2(\gamma+\kappa)}) + n^6 \exp(-c_2 n^\gamma)] + o(1).$$

If Condition (C6) also holds, we have

$$\mathbb{P}(\mathcal{A} \subseteq \hat{\mathcal{M}}_{d_n}) \geq 1 - |\mathcal{A}| [\exp(-c_1 n^{1-2(\gamma+\kappa)}) + n^6 \exp(-c_2 n^\gamma) + \exp(-c_3 n^{1-2\kappa})] + o(1),$$

$$\mathbb{P}(\hat{\mathcal{M}}_{d_n} \subseteq \mathcal{A}) \geq 1 - d_n [\exp(-c_1 n^{1-2(\gamma+\kappa)}) + n^6 \exp(-c_2 n^\gamma) + \exp(-c_3 n^{1-2\kappa})] + o(1),$$

where $|\mathcal{A}|$ is the size of the set \mathcal{A} and c_3 is a positive constant. If $\log p = O(n^{\min\{1-2(\gamma+\kappa), \gamma\}})$, then the strong screening consistency holds,

$$\mathbb{P}(\hat{\mathcal{M}}_{d_n} = \mathcal{A}) \xrightarrow{a.s.} 1 \text{ when } n \rightarrow \infty.$$

Theorem 3 claims that, without specifying a model among X_r, Y , and Z , the COME-CSIS enjoys the strong screening property for the directionally limited metric space-valued response. Thus, it works for data in typical non-Euclidean spaces like separable Banach spaces, Riemannian manifolds, etc. The COME-CSIS imposes no moment assumption on X_1, \dots, X_p and Y , and thus, it is robust to heavy-tailed observations and the presence of potential outliers appearing in these variables. This property is beneficial for high-dimensional

data analysis because it is rigorous to assume all explanatory variables are well-behavior when p is large.

As a complementary, we discuss determining the model size d_n . Generally speaking, it involves conducting a conditional independence test, a tough hypothesis test (Shah and Peters, 2020). Fortunately, if we assume the dependence between Y and (X, Z) follows one of the models: global Fréchet regression (Petersen and Müller, 2019), geodesic regression (Fletcher, 2013) or intrinsic regression (Cornea et al., 2016), then we could stop adding a new predictor when it does not statistically affect the interpretation of the variation of Y . This effect can be measured by a generalization of the adjusted coefficient of determination for the global Fréchet regression and geodesic regression, or a Wald-type test statistic for the intrinsic regression model.

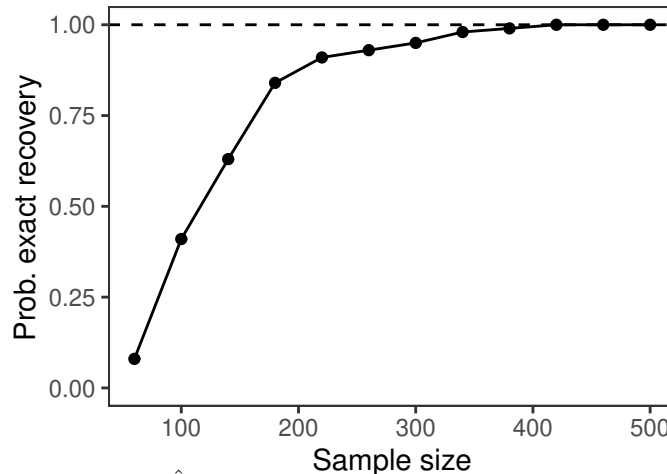


Fig 1: Plot of the probability $\mathbb{P}(\hat{\mathcal{M}}_{d_n} = \mathcal{A})$ versus the sample size under Model (1.b) described in Section 5.1.

4. Screening of Corpus Callosum Shape. Imaging genetics has gradually become an up-and-coming field. Combining genetics and functional neuroimaging allows scientists to detect the association between neuroimaging phenotype and genetic variation. In this section, we analyze databases with imaging, genetic, and clinical data provided by the Alzheimer’s Disease Neuroimaging Initiative (ADNI) study¹ to demonstrate the helpfulness of the COME-CSIS.

The corpus callosum (CC) is the largest white matter structure in the human brain, connecting the left and right hemispheres in the brain (Edwards et al., 2014). Anatomically, CC is roughly a 10 cm long, 1 cm wide curved structure in an adult human, containing approximately 200 million fibers. Standard anatomic divisions for CC are the rostrum, genu, body (including anterior and posterior parts), isthmus, and splenium (see Figure 2). Functionally, CC is essential for communication between the two cerebral hemispheres. It facilitates the integration of sensory and motor information from the two sides of the body and different influences on higher cognition related to social interaction and language. Since CC is an essential structural and functional part of the brain, finding the factors that impact its shape is valuable. Existing literature has shown that age and disease are related to CC shape (Hinkle, Fletcher and Joshi, 2014; Cornea et al., 2016; Fletcher, 2013; Joshi et al., 2013); However, the genetic factors influencing the CC shape have been largely undiscovered.

¹adni.loni.usc.edu

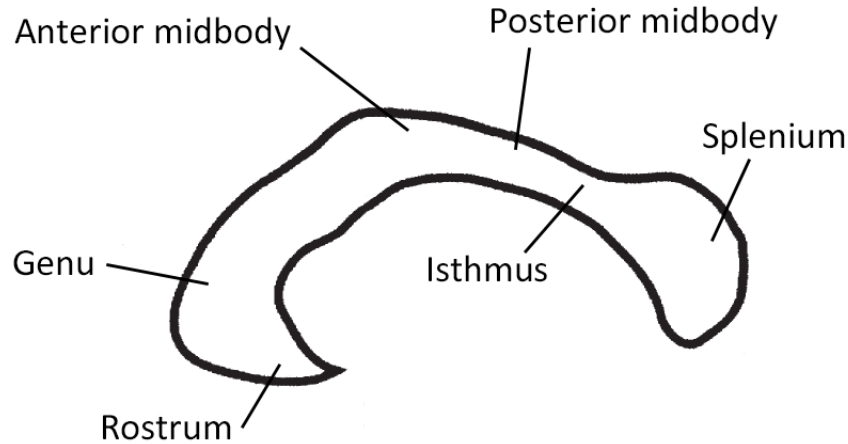


Fig 2: The image of midsagittal cut through the corpus callosum in [Eccher \(2014\)](#) with its major subunits from anterior to posterior: rostrum, genu, anterior midbody, posterior midbody, isthmus, and splenium.

To this end, we analyze a preprocessed ADNI dataset ([Cornea et al., 2016](#)) containing CC shapes and demographics. The preprocessed dataset includes 371 subjects, where each subject's gender, age, disease diagnosis (AD or health), CC's shape and 6,995 single nucleotide polymorphisms (SNPs) are recorded. 50 two-dimensional points characterize the CC shape of each subject on the CC contour. Moreover, the dissimilarity between two shape observations are measured by Riemannian shape distance ([Dryden and Mardia, 2016](#)).

Next, we specify the explanatory variables and conditional variables in our analysis. Due to the difference in shape along the inner side of the posterior splenium and isthmus subregions for different age groups, it is concluded that age strongly influences the shape of CC contours ([Cornea et al., 2016](#)). Besides, [Cornea et al. \(2016\)](#) points out that the splenium seems less rounded, and the isthmus is thinner in subjects with AD than in HC. Given the two prior information, our interest is to detect the genetic factors associated with CC contour when controlling covariates age and group. Moreover, to verify the arguments that there is no significant gender effect on the CC shape after disease status and age are considered ([Cornea et al., 2016](#)), we treat gender as one of the explanatory variables in the screening procedure.

Table 1 lists the top 5 important SNPs selected for CC shape by the BCor-SIS, CDC-SIS, and COME-CSIS. From Table 1, the COME-CSIS and CDC-SIS select similar top-5 SNPs, but BCor-SIS selects quite different SNPs, This implies that considering the conditional variable greatly impacts the screening results. The SNP rs11668269, selected by the COME-CSIS and CDC-SIS, is in the LOC105372330 gene that is negatively correlated to APOE4+ males frontal white matter, where the APOE4 allele causes damage to the white matter of the corpus callosum ([Hsu et al., 2019](#); [Koizumi et al., 2018](#)).

The SNP rs4807022, initially identified through BCor-SIS, is within the gene encoding protein tyrosine phosphatase receptor sigma (PTPRS). This placement suggests a significant association with the CC shape. We conducted a hypothesis test on SNP rs4807022 with the conditional variables to further explore this relationship, employing Ball Covariance. The analysis yielded a p-value of 0.0267 for the association between the SNP and age, indicating a strong correlation. Conversely, the p-value for the association between the SNP and Alzheimer's Disease (AD) was 0.99, suggesting no significant dependence. We then seg-

mented the data into age groups based on quantiles (55–72, 73–76, 77–80, and 81–95²) to examine variations across different age segments. This SNP data categorizes genetic variations as 0 (AA), 1 (Aa), and 2 (aa), representing two, one, and zero copies of the reference allele, respectively. The results, summarized in Table 2, reveal that the frequency of heterozygotes (1 for genotype Aa) increases with age. PTPRS has been implicated in the regulation of neurite outgrowth and has been shown to stimulate neurite outgrowth in response to the heparan sulfate proteoglycan GPC2, essential for normal brain development (Pulido et al., 1995; Coles et al., 2011). These functions suggest that PTPRS may play a role in longevity. Despite these findings, SNP rs4807022 is ranked 4808th in COME-CSIS, and when conditioned on age, the p-value derived from the COME analysis is 0.37. Overall, while there is a strong association between SNP rs4807022 and age, its link to CC shape appears to be mediated primarily through age-related changes rather than a direct genetic influence on CC shape.

Moreover, the COME-CSIS selects the SNP rs3745129 in the ZNF329 gene as the fourth important gene. Because an important paralog of the ZNF329 gene, ZFP37, expresses in all neurons of the central nervous system (Mazarakis et al., 1996), ZNF329 may influence the corpus callosum. Finally, the gender factor is ranked 4553 by the COME-CSIS, implying the gender effect is not significant after considering the age and disease status. This result is coincident with the finding of Cornea et al. (2016).

To further compare the performance of COME-CSIS and CDC-SIS, we randomly generated 1,000 noise SNP variables and identified the proportion of noise selected by the two methods. Specifically, we randomly generated the probability of 0, 1, and 2 and then generated noise SNPs according to the multivariate distribution. The experiment was repeated 20 times, and we selected 10, 20, 50, and 100 variables as references. The results in Table 3 demonstrate that the COME-CSIS method selects a higher proportion of original, non-noise SNPs than CDC-SIS. This indicates that COME-CSIS is more robust and less affected by noise in the data.

TABLE 1
Top-5 selected variables for corpus callosum shape by different methods. SNP's corresponding genes are in parentheses if they exist.

BCor-SIS	CDC-SIS	COME-CSIS
rs4807022 (PTPRS)	rs10414182	rs11668269 (LOC105372330)
rs8101539 (WDR88)	rs10424248	rs10414182
rs3786627 (ETFB)	rs11668269 (LOC105372330)	rs3786776 (PLA2G4C)
rs11085313	rs1979260 (MYO9B)	rs3745129 (ZNF329)
rs4805863	rs3786776 (PLA2G4C)	rs10518253

TABLE 2
SNP value in four age groups.

	55–72	73–76	77–80	81–95
AA	70	72	65	50
Aa	35	13	25	33
aa	1	2	2	2

We visualize CC shapes in Figure 3 to gain more insight. Specifically, we divide the subjects into eight disjoint subsets according to their ages phase (55–72, 73–76, 77–80, and

²55, 72, 76, 80, and 92 are 0.0, 0.25, 0.5, 0.75, and 1.0 quantiles of the age, respectively.

TABLE 3
The average proportion of original SNPs selected by the two methods.

	10	20	50	100
COME-CSIS	58.75%	61.86%	71.75%	70%
CDC-SIS	33.75%	41.86%	54.25%	52.36%

81–95³) and disease status (AD and HC), then, in each part of the subject, we demonstrate the Fréchet mean of CC shapes when the genetic factor takes different values. It can be observed that, for both of the top-2 SNPs selected by the COME-CSIS, they impact the CC shape condition on age and health status. More precisely, for the healthy subjects with age 72–76, the SNP rs11668269 with value AA associates with a smaller curvature in the body part of CC; for the AD patients with age 72–76, the SNP rs10410302 with value AA leads to a smaller curvature in the body part of CC.

In practical applications, COME-CSIS demonstrates enhanced capability in identifying key variables compared to methods that do not utilize conditional variables. By preemptively controlling for confounding factors such as age and gender, COME-CSIS allows for more accurate isolation and identification of core variables. Compared with other conditional variable screening methods (CDC-SIS), the COME-CSIS is more robust and less likely to select irrelevant noise. Consequently, this approach improves the robustness and reliability of the findings in complex analytical scenarios where multiple interdependent variables are present.

5. Simulation. In this section, we investigate the empirical performance of the COME-CSIS by synthesis datasets. We evaluate the COME-CSIS by the proportion P_i that it correctly includes the effective variable X_i under a given model size d_n in the R replications (Li, Zhong and Zhu, 2012). We also consider the proportion P_a that all effective variables are selected simultaneously. If the screening procedure works well, P_i s and P_a should be close to 1. We fix the sample size n at 150, the dimension p at 2000, and the number of replications R at 100. We set the model size $d = \gamma \lceil n / \log(n) \rceil$ as Li, Zhong and Zhu (2012) suggested, where $\lceil a \rceil$ refers to the integer part of a and γ 's value is 1, 2, or 3. For comparison, the BCorSIS (Pan et al., 2019) and CDC-SIS (Wang et al., 2017) are taken into consideration, and two R packages: Ball and cdcsis (Zhu et al., 2021; Hu et al., 2019) are used to perform the two screening procedures. Since the CDC-SIS also relies on kernel density estimation, for fairness, the kernel function and its bandwidth used in the CDC-SIS is controlled to be the same as that of the COME-CSIS.

We consider two common data types of non-Euclidean response: functional data and directional data, in Section 5.1 and Section 5.2, respectively. As a complementary, the study of the classical Euclidean response is deferred to the supplementary material. For the conditional variable and explanatory variables (Z, X_1, \dots, X_p) , they are jointly sampled from a multivariate normal distribution with zero means and covariance matrix Σ where $\Sigma_{ij} = 2\rho^{|i-j|}$. The value of ρ may be 0.0 or 0.7.

5.1. Functional curve data. First, we entail the procedure for synthesizing the functional curve response. Suppose $B_1(t), \dots, B_4(t)$ are four B-spline basis functions, we generate the a response Y as the linear combination of the basis functions, where the linear coefficients are related to Z, X_1, X_3, X_6 . We consider the following two models. The first model is a generalized additive model, and the second one is an interaction model:

$$(1.a): Y(t) = ZB_1(t) + X_1B_2(t) + X_3B_3(t) + X_6^2B_4(t) + \epsilon(t);$$

$$(1.b): Y(t) = ZB_1(t) + 2X_1X_3B_2(t) + ZX_3B_3(t) + ZX_6B_4(t) + \epsilon(t).$$

³55, 72, 76, 80, and 92 are 0.0, 0.25, 0.5, 0.75, and 1.0 quantiles of the age, respectively.

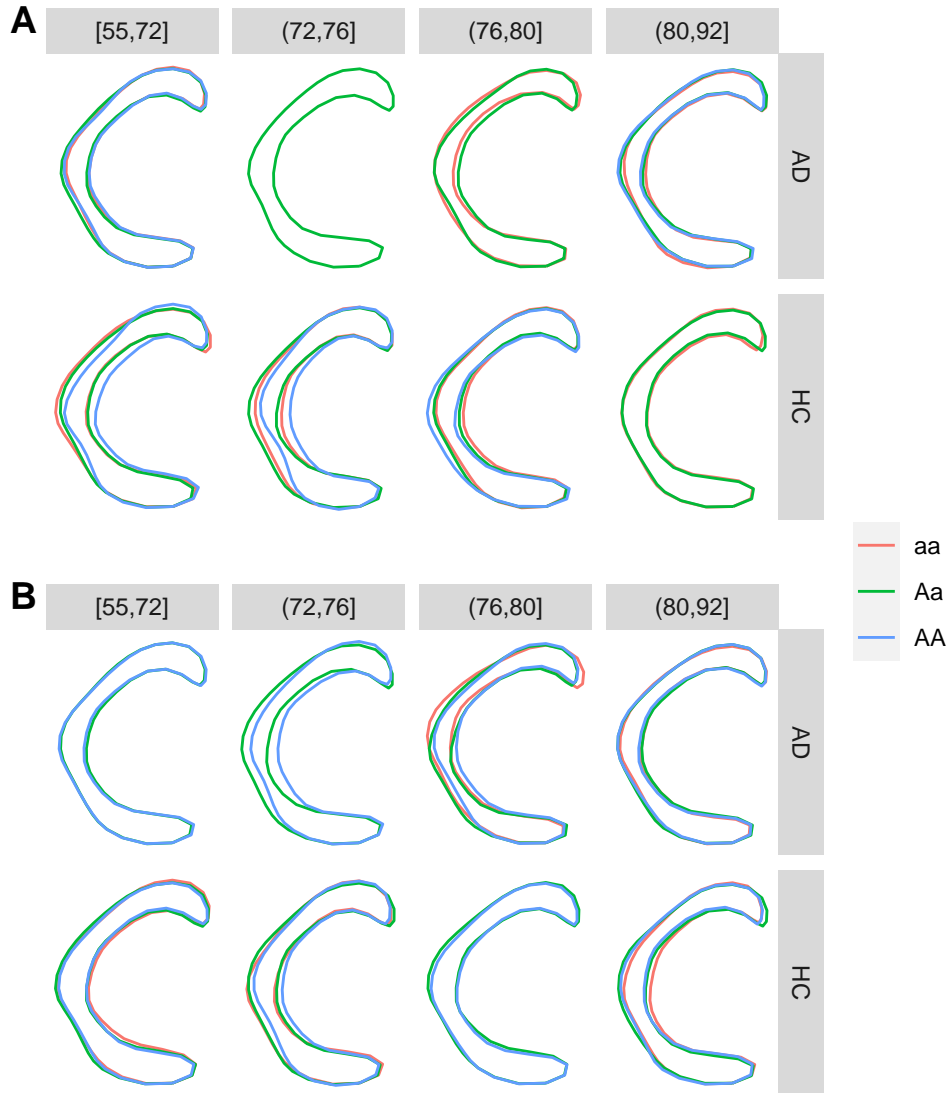


Fig 3: The corpus callosum (CC) shape in SNP rs11668269 (subfigure A) and rs10410302 (subfigure B). In each subfigure, the lower panels indicate healthy control, the upper panels indicate patients with Alzheimer’s disease, and a column represents a specific age group. Four columns represent 55–72, 73–76, 77–80, and 81–95 years old, respectively. Ordinary Procrustes analysis (Dryden and Mardia, 2016) are conducted for all CC shapes.

$\epsilon(t)$ is a zero-mean Gaussian process in these two models. The functional curve $Y(t)$ is observed in 17 equally spaced points at interval $[0, 8\pi]$. To conduct the three screening procedures, L_2 norm (Febrero-Bande and de la Fuente, 2012) are used to measure the dissimilarity of two functional observations.

The results on functional data are displayed in Table 4. For Model (1. a), the three methods have a high probability of identifying the true variables, and both CDC-SIS and BCor-SIS are slightly better than the COME-CSIS. The CDC-SIS surpasses COME-CSIS because distance correlation-based methods have strong power in detecting the linear relationship (Pan et al., 2020); BCor-SIS has better power because the effect of the conditional variable Z can be considered additive noise. In Model (1. b), the COME-CSIS turns into the most powerful

method and has a much larger chance to detect all influential variables simultaneously when $\rho = 0$. It is also worth noting that BCor-SIS has limited power to detect the influential variable X_6 that interacts with the conditional variable.

TABLE 4
The selection proportion of effective variables in functional data.

ρ	γ	Methods	Model (1.a)				Model (1.b)			
			P_1	P_3	P_6	P_a	P_1	P_3	P_6	P_a
0.0	d_1	CDC-SIS	1.00	1.00	1.00	1.00	0.75	0.99	1.00	0.75
	d_2	BCor-SIS	1.00	0.99	1.00	0.99	0.93	1.00	0.48	0.43
	d_3	COME-CSIS	0.97	0.93	1.00	0.90	0.97	1.00	1.00	0.97
	d_1	CDC-SIS	1.00	1.00	1.00	1.00	0.83	1.00	1.00	0.83
	d_2	BCor-SIS	1.00	1.00	1.00	1.00	0.96	1.00	0.61	0.58
	d_3	COME-CSIS	0.99	0.97	1.00	0.96	0.98	1.00	1.00	0.98
	d_1	CDC-SIS	1.00	1.00	1.00	1.00	0.88	1.00	1.00	0.88
	d_2	BCor-SIS	1.00	1.00	1.00	1.00	0.98	1.00	0.71	0.69
	d_3	COME-CSIS	0.99	0.98	1.00	0.97	0.98	1.00	1.00	0.98
0.7	d_1	CDC-SIS	1.00	1.00	1.00	1.00	1.00	1.00	1.00	1.00
	d_2	BCor-SIS	1.00	1.00	1.00	1.00	1.00	1.00	0.51	0.51
	d_3	COME-CSIS	0.96	1.00	1.00	0.96	0.99	1.00	1.00	0.99
	d_1	CDC-SIS	1.00	1.00	1.00	1.00	1.00	1.00	1.00	1.00
	d_2	BCor-SIS	1.00	1.00	1.00	1.00	1.00	1.00	0.60	0.60
	d_3	COME-CSIS	0.97	1.00	1.00	0.97	1.00	1.00	1.00	1.00
	d_1	CDC-SIS	1.00	1.00	1.00	1.00	1.00	1.00	1.00	1.00
	d_2	BCor-SIS	1.00	1.00	1.00	1.00	1.00	1.00	0.71	0.71
	d_3	COME-CSIS	0.99	1.00	1.00	0.99	1.00	1.00	1.00	1.00

5.2. *Directional data.* We consider two models for generating directional data. The first model generates observations in a unit sphere, while the second generates observations in a unit circle. In the following, $U_c(a, b)$ represents a uniform distribution on the unit circle, where a and b are the lower and upper bound of the radian. The two models are:

$$(2.a): \quad \phi = ZX_3, \theta = \frac{1}{2}(X_6 + X_9)$$

$$Y = (\sin \theta \cos \phi, \cos \theta \sin \phi, \cos \theta).$$

(2.b): $\omega_1, \omega_2, \omega_3$ are *i.i.d* Bernoulli random variables with $\frac{1}{2}$ probability to take value 1,

$$Y = \begin{cases} \omega_1 U_c(0, \frac{\pi}{6}) + (1 - \omega_1) U_c(\pi, \frac{7\pi}{6}), & \text{if } Z' = 1, X'_3 = I(X_3 > \text{median}(X_3)) \\ \omega_1 U_c(\frac{\pi}{2}, \frac{2\pi}{3}) + (1 - \omega_1) U_c(\frac{3\pi}{2}, \frac{5\pi}{3}), & \text{if } Z' = 1, X'_3 = I(X_3 \leq \text{median}(X_3)) \\ \omega_2 U_c(\frac{\pi}{6}, \frac{\pi}{3}) + (1 - \omega_2) U_c(\frac{7\pi}{6}, \frac{4\pi}{3}), & \text{if } Z' = 2, X'_6 = I(X_6 > \text{median}(X_6)) \\ \omega_2 U_c(\frac{2\pi}{3}, \frac{5\pi}{6}) + (1 - \omega_2) U_c(\frac{5\pi}{3}, \frac{11\pi}{6}), & \text{if } Z' = 2, X'_6 = I(X_6 \leq \text{median}(X_6)) \\ \omega_3 U_c(\frac{\pi}{3}, \frac{\pi}{2}) + (1 - \omega_3) U_c(\frac{4\pi}{3}, \frac{3\pi}{2}), & \text{if } Z' = 3, X'_9 = I(X_9 > \text{median}(X_9)) \\ \omega_3 U_c(\frac{5\pi}{6}, \pi) + (1 - \omega_3) U_c(\frac{11\pi}{6}, 2\pi), & \text{if } Z' = 3, X'_9 = I(X_9 \leq \text{median}(X_9)) \end{cases},$$

where $Z' = I(Z \leq z^{\frac{1}{3}}) + 2I(z^{\frac{1}{3}} < Z \leq z^{\frac{2}{3}}) + 3I(z^{\frac{2}{3}} > Z)$, and $z^{\frac{1}{3}}, z^{\frac{2}{3}}$ are $\frac{1}{3}$ and

$\frac{2}{3}$ quantiles of Z , respectively.

The geodesic distance measures the dissimilarity of two directional observations.

The performances of the three screening procedures on Models (2.a) and (2.b) are exhibited in Table 5. From the results of (2.a) in Table 5, all methods are powerful in identifying the variables X_6, X_9 that have no interaction with the conditional variable; however, only the COME-CSIS is good at detecting the effective variable X_3 that has an interaction effect on Y . Furthermore, under Model (2.b), the CDC-SIS cannot select all influential variables simultaneously since distance covariance works on metric space satisfying a strong negative type condition (Lyons, 2013). Nevertheless, the COME-CSIS and BCor-SIS still have powerful performance, generally surpassing the BCor-SIS.

TABLE 5
The selection proportion of effective variables in directional data.

ρ	γ	Methods	Model (2.a)				Model (2.b)			
			P_3	P_6	P_9	P_a	P_3	P_6	P_9	P_a
0.0	d_1	CDC-SIS	0.64	0.99	0.99	0.62	0.04	0.00	0.00	0.00
	d_2	BCor-SIS	0.06	1.00	1.00	0.06	0.39	0.31	0.35	0.04
	d_3	COME-CSIS	0.96	0.92	0.96	0.85	0.76	0.70	0.69	0.36
	d_1	CDC-SIS	0.77	0.99	1.00	0.76	0.05	0.01	0.01	0.00
	d_2	BCor-SIS	0.08	1.00	1.00	0.08	0.59	0.48	0.54	0.18
	d_3	COME-CSIS	0.98	0.95	0.98	0.91	0.92	0.84	0.83	0.64
	d_1	CDC-SIS	0.83	1.00	1.00	0.83	0.07	0.01	0.01	0.00
	d_2	BCor-SIS	0.11	1.00	1.00	0.11	0.73	0.59	0.65	0.30
	d_3	COME-CSIS	0.99	0.97	0.99	0.95	0.94	0.90	0.92	0.78
0.7	d_1	CDC-SIS	0.61	1.00	1.00	0.61	0.01	0.01	0.01	0.00
	d_2	BCor-SIS	0.08	1.00	1.00	0.08	0.55	0.69	0.65	0.25
	d_3	COME-CSIS	0.93	1.00	0.99	0.93	0.54	0.79	0.81	0.37
	d_1	CDC-SIS	0.76	1.00	1.00	0.76	0.01	0.03	0.02	0.00
	d_2	BCor-SIS	0.15	1.00	1.00	0.15	0.75	0.87	0.83	0.55
	d_3	COME-CSIS	0.96	1.00	1.00	0.96	0.71	0.91	0.90	0.59
	d_1	CDC-SIS	0.80	1.00	1.00	0.80	0.02	0.05	0.03	0.00
	d_2	BCor-SIS	0.20	1.00	1.00	0.20	0.86	0.92	0.91	0.72
	d_3	COME-CSIS	0.96	1.00	1.00	0.96	0.79	0.96	0.92	0.71

6. Conclusion and Discussion. We develop a related model/distribution-free COME-CSIS method to detect genes related to the corpus callosum, and propose a novel conditional dependence measure, COME, to identify potentially important features given confounders.

Our method is universal and widely applicable because strong negative type and moment conditions do not restrict it required by other popular conditional sure independence screening procedures. The non-asymptotic property of the COME-CSIS and the convergence rate of its sure property are also rigorously investigated. In the application part, COME-CSIS shows improved identification of key variables over methods that do not use conditional variables by controlling confounders like age and gender. It more accurately isolates core variables and is more robust than other methods, reducing the selection of irrelevant noise.

Moreover, from our numerical study, the COME-CSIS is talented at unveiling explanatory variables with non-linear response relationships, especially when conditional variables and affective variables interact with the response.

Finally, we provide an iterative version of the COME-CSIS procedure that can be developed to gain more power when explanatory variables are correlated. The procedure is summarized in the following.

1. Apply the COME-CSIS method on the response Y and predictors X when considering conditional variables Z , and suppose the r_i -th predictor has the largest COME.

2. Update the set of conditional variables and explanatory variables:

$$X \leftarrow X \setminus X_{r_i}, Z \leftarrow Z \cup X_{r_i}.$$

3. Repeat Steps 1 and 2 until the selected predictors exceed the prespecified number s .

A vital advantage of the I-COME-CSIS procedure is that it exploits the information supplied by selected predictors. Imaging that irrelevant variables gain predictive power from a strong dependence on the active variables. This iterative procedure reduces irrelevant variables' predictive power on the shape response once their correlated active variables are selected. Furthermore, the I-COME-CSIS can enhance the detection of the rest of the active variables. The challenge of the procedure is that the kernel density estimation for Z is difficult when it is high dimensional, and recently advanced kernel density estimation technique (Liu et al., 2021) may be helpful in this case.

Acknowledgments. Dr. Wang's research is partially supported by NSFC (11771462, 71991474). Dr. Pan's research is partially supported by NSFC (11701590), Science Foundation of Guangdong Province of China (2017A030310053), and Young Teacher Program/Fundamental Research Funds for the Central Universities (17lgpy14).

Data collection and sharing for this project was funded by the Alzheimer's Disease Neuroimaging Initiative (ADNI) (National Institutes of Health Grant U01 AG024904) and DOD ADNI (Department of Defense award number W81XWH-12-2-0012). ADNI is funded by the National Institute on Aging, the National Institute of Biomedical Imaging and Bioengineering, and through generous contributions from the following: AbbVie, Alzheimer's Association; Alzheimer's Drug Discovery Foundation; Araclon Biotech; BioClinica, Inc.; Biogen; Bristol-Myers Squibb Company; CereSpir, Inc.; Cogstate; Eisai Inc.; Elan Pharmaceuticals, Inc.; Eli Lilly and Company; EuroImmun; F. Hoffmann-La Roche Ltd and its affiliated company Genentech, Inc.; Fujirebio; GE Healthcare; IXICO Ltd.; Janssen Alzheimer Immunotherapy Research & Development, LLC.; Johnson & Johnson Pharmaceutical Research & Development LLC.; Lumosity; Lundbeck; Merck & Co., Inc.; Meso Scale Diagnostics, LLC.; NeuroRx Research; Neurotrack Technologies; Novartis Pharmaceuticals Corporation; Pfizer Inc.; Piramal Imaging; Servier; Takeda Pharmaceutical Company; and Transition Therapeutics. The Canadian Institutes of Health Research is providing funds to support ADNI clinical sites in Canada. Private sector contributions are facilitated by the Foundation for the National Institutes of Health (www.fnih.org). The grantee organization is the Northern California Institute for Research and Education, and the study is coordinated by the Alzheimer's Therapeutic Research Institute at the University of Southern California. ADNI data are disseminated by the Laboratory for Neuro Imaging at the University of Southern California.

SUPPLEMENTARY MATERIAL

Supplement A: Supplement for "Identification of Genetic Factors Associated with Corpus Callosum Morphology: Conditional Strong Independence Screening for Non-Euclidean Responses"

The Supplementary Material includes technical proof, implementation details, and the detail of the iterative COME-CSIS algorithm.

Supplement B: R code for "Identification of Genetic Factors Associated with Corpus Callosum Morphology: Conditional Strong Independence Screening for Non-Euclidean Responses"

R-package *come* containing code to perform the COME-CSIS described in the article and R scripts used to generate the numerical results presented in the manuscript.

REFERENCES

- BACHMAN, A. H., LEE, S. H., SIDTIS, J. J. and ARDEKANI, B. A. (2014). Corpus callosum shape and size changes in early Alzheimer's disease: A longitudinal MRI study using the OASIS brain database. *Journal of Alzheimer's Disease* **39** 71–78.
- BARUT, E., FAN, J. and VERHASSELT, A. (2016). Conditional Sure Independence Screening. *Journal of the American Statistical Association* **111** 1266–1277. PMID: 28360436. <https://doi.org/10.1080/01621459.2015.1092974>
- BISWAL, B. B., MENNES, M., ZUO, X.-N., GOHEL, S., KELLY, C., SMITH, S. M., BECKMANN, C. F., ADELSTEIN, J. S., BUCKNER, R. L., COLCOMBE, S., DOGONOWSKI, A.-M., ERNST, M., FAIR, D., HAMPSON, M., HOPTMAN, M. J., HYDE, J. S., KIVINIEMI, V. J., KÖTTER, R., LI, S.-J., LIN, C.-P., LOWE, M. J., MACKAY, C., MADDEN, D. J., MADSEN, K. H., MARGULIES, D. S., MAYBERG, H. S., MCMAHON, K., MONK, C. S., MOSTOFISKY, S. H., NAGEL, B. J., PEKAR, J. J., PELTIER, S. J., PETERSEN, S. E., RIEDL, V., ROMBOUITS, S. A. R. B., RYPMA, B., SCHLAGGAR, B. L., SCHMIDT, S., SEIDLER, R. D., SIEGLE, G. J., SORG, C., TENG, G.-J., VEIJOLA, J., VILLRINGER, A., WALTER, M., WANG, L., WENG, X.-C., WHITFIELD-GABRIELI, S., WILLIAMSON, P., WINDISCHBERGER, C., ZANG, Y.-F., ZHANG, H.-Y., CASTELLANOS, F. X. and MILHAM, M. P. (2010). Toward discovery science of human brain function. *Proceedings of the National Academy of Sciences* **107** 4734–4739. <https://doi.org/10.1073/pnas.0911855107>
- CHEN, X., ZHANG, Y., CHEN, X. and LIU, Y. (2019). A simple model-free survival conditional feature screening. *Statistics & Probability Letters* **146** 156–160.
- COLES, C. H., SHEN, Y., TENNEY, A. P., SIEBOLD, C., SUTTON, G. C., LU, W., GALLAGHER, J. T., JONES, E. Y., FLANAGAN, J. G. and ARICESCU, A. R. (2011). Proteoglycan-specific molecular switch for RPTP α clustering and neuronal extension. *Science* **332** 484–488.
- CORNEA, E., ZHU, H., KIM, P. and IBRAHIM, J. (2016). Regression Models on Riemannian Symmetric Spaces. *Journal of the Royal Statistical Society: Series B (Statistical Methodology)* **79** n/a-n/a. <https://doi.org/10.1111/rssb.12169>
- DRYDEN, I. L. and MARDIA, K. V. (2016). *Statistical shape analysis: with applications in R* **995**. John Wiley & Sons.
- ECCHER, M. (2014). Corpus Callosum. In *Encyclopedia of the Neurological Sciences (Second Edition)* second edition ed. (M. J. Aminoff and R. B. Daroff, eds.) 867 - 868. Academic Press, Oxford. <https://doi.org/10.1016/B978-0-12-385157-4.01137-4>
- EDWARDS, T. J., SHERR, E. H., BARKOVICH, A. J. and RICHARDS, L. J. (2014). Clinical, genetic and imaging findings identify new causes for corpus callosum development syndromes. *Brain* **137** 1579–1613. <https://doi.org/10.1093/brain/awt358>
- FAN, J. and LV, J. (2008). Sure independence screening for ultrahigh dimensional feature space. *Journal of the Royal Statistical Society: Series B (Statistical Methodology)* **70** 849–911. <https://doi.org/10.1111/j.1467-9868.2008.00674.x>
- FEBRERO-BANDE, M. and DE LA FUENTE, M. (2012). Statistical Computing in Functional Data Analysis: The R Package *fda.usc*. *Journal of Statistical Software, Articles* **51** 1–28. <https://doi.org/10.18637/jss.v051.i04>
- FEDERER, H. (2014). *Geometric measure theory*. Springer.
- FLETCHER, P. T. (2013). Geodesic regression and the theory of least squares on Riemannian manifolds. *International journal of computer vision* **105** 171–185.
- FUKUMIZU, K., GRETTON, A., SUN, X. and SCHÖLKOPF, B. (2008). Kernel measures of conditional dependence. In *Advances in neural information processing systems* 489–496.
- HINKLE, J., FLETCHER, P. T. and JOSHI, S. (2014). Intrinsic polynomials for regression on Riemannian manifolds. *Journal of Mathematical Imaging and Vision* **50** 32–52.
- HONG, H. G., KANG, J. and LI, Y. (2018). Conditional screening for ultra-high dimensional covariates with survival outcomes. *Lifetime data analysis* **24** 45–71.
- HONG, H. G., WANG, L. and HE, X. (2016). A data-driven approach to conditional screening of high-dimensional variables. *Stat* **5** 200–212.
- HSU, M., DEDHIA, M., CRUSIO, W. and DELPRATO, A. (2019). Sex differences in gene expression patterns associated with the APOE4 allele. *F1000Research* **8**. <https://doi.org/10.12688/f1000research.18671.2>
- HU, Q. and LIN, L. (2017). Conditional sure independence screening by conditional marginal empirical likelihood. *Annals of the Institute of Statistical Mathematics* **69** 63–96.
- HU, W., HUANG, M., PAN, W., WANG, X., WEN, C., TIAN, Y., ZHANG, H. and ZHU, J. (2019). *cdsis: Conditional Distance Correlation Based Feature Screening and Conditional Independence Inference R package version 2.0.3*.

- HUANG, D., LI, R. and WANG, H. (2014). Feature Screening for Ultrahigh Dimensional Categorical Data With Applications. *Journal of Business & Economic Statistics* **32** 237-244. <https://doi.org/10.1080/07350015.2013.863158>
- JOSHI, S. H., NARR, K. L., PHILIPS, O. R., NUECHTERLEIN, K. H., ASARNOW, R. F., TOGA, A. W. and WOODS, R. P. (2013). Statistical shape analysis of the corpus callosum in schizophrenia. *Neuroimage* **64** 547-559.
- KENNEDY, H., VAN ESSEN, D. C. and CHRISTEN, Y. (2016). *Micro-, meso-and macro-connectomics of the brain*. Springer Nature.
- KOIZUMI, K., HATTORI, Y., AHN, S. J., BUENDIA, I., CIACCIARELLI, A., UEKAWA, K., WANG, G., HILLER, A., ZHAO, L., VOSS, H. U. et al. (2018). Apo ϵ 4 disrupts neurovascular regulation and undermines white matter integrity and cognitive function. *Nature communications* **9** 1-11.
- LI, R., ZHONG, W. and ZHU, L. (2012). Feature Screening via Distance Correlation Learning. *Journal of the American Statistical Association* **107** 1129-1139. PMID: 25249709. <https://doi.org/10.1080/01621459.2012.695654>
- LIN, L. and SUN, J. (2016). Adaptive conditional feature screening. *Computational Statistics & Data Analysis* **94** 287 - 301. <https://doi.org/10.1016/j.csda.2015.09.002>
- LIU, Y. and CHEN, X. (2018). Quantile screening for ultra-high-dimensional heterogeneous data conditional on some variables. *Journal of Statistical Computation and Simulation* **88** 329-342.
- LIU, J., LI, R. and WU, R. (2014). Feature selection for varying coefficient models with ultrahigh-dimensional covariates. *Journal of the American Statistical Association* **109** 266-274.
- LIU, Q., XU, J., JIANG, R. and WONG, W. H. (2021). Density estimation using deep generative neural networks. *Proceedings of the National Academy of Sciences* **118**. <https://doi.org/10.1073/pnas.2101344118>
- LU, S., CHEN, X. and WANG, H. (2019). Conditional distance correlation sure independence screening for ultrahigh dimensional survival data. *Communications in Statistics-Theory and Methods* 1-18.
- LYONS, R. (2013). Distance Covariance in Metric Spaces. *The Annals of Probability* **41** 3284-3305. <https://doi.org/10.1214/12-AOP803>
- MAZARAKIS, N., MICHALOVICH, D., KARIS, A., GROSVELD, F. and GALJART, N. (1996). Zfp-37Is a Member of the KRAB Zinc Finger Gene Family and Is Expressed in Neurons of the Developing and Adult CNS. *Genomics* **33** 247-257. <https://doi.org/10.1006/geno.1996.0189>
- MEINSHAUSEN, N. and BUHLMANN, P. (2006). High-dimensional graphs and variable selection with the Lasso. *Ann. Statist.* **34** 1436-1462. <https://doi.org/10.1214/009053606000000281>
- PAN, W., WANG, X., XIAO, W. and ZHU, H. (2019). A generic sure independence screening procedure. *Journal of the American Statistical Association* **114** 928-937.
- PAN, W., WANG, X., ZHANG, H., ZHU, H. and ZHU, J. (2020). Ball Covariance: A Generic Measure of Dependence in Banach Space. *Journal of the American Statistical Association* **115** 307-317. <https://doi.org/10.1080/01621459.2018.1543600>
- PETERSEN, A. and MÜLLER, H.-G. (2019). Fréchet regression for random objects with Euclidean predictors. *Ann. Statist.* **47** 691-719. <https://doi.org/10.1214/17-AOS1624>
- PULIDO, R., SERRA-PAGES, C., TANG, M. and STREULI, M. (1995). The LAR/PTP delta/PTP sigma subfamily of transmembrane protein-tyrosine-phosphatases: multiple human LAR, PTP delta, and PTP sigma isoforms are expressed in a tissue-specific manner and associate with the LAR-interacting protein LIP. 1. *Proceedings of the National Academy of Sciences* **92** 11686-11690.
- SHAH, R. D. and PETERS, J. (2020). The hardness of conditional independence testing and the generalised covariance measure. *Annals of Statistics* **48** 1514-1538. <https://doi.org/10.1214/19-AOS1857>
- TANAKA-ARAKAWA, M. M., MATSUI, M., TANAKA, C., UEMATSU, A., UDA, S., MIURA, K., SAKAI, T. and NOGUCHI, K. (2015). Developmental changes in the corpus callosum from infancy to early adulthood: a structural magnetic resonance imaging study. *PLoS one* **10** e0118760.
- VERMEULEN, C. L., DU TOIT, P. J., VENTER, G. and HUMAN-BARON, R. (2023). A morphological study of the shape of the corpus callosum in normal, schizophrenic and bipolar patients. *Journal of anatomy* **242** 153-163.
- WANG, X., PAN, W., HU, W., TIAN, Y. and ZHANG, H. (2015). Conditional Distance Correlation. *Journal of the American Statistical Association* **110** 1726-1734. PMID: 26877569. <https://doi.org/10.1080/01621459.2014.993081>
- WANG, X., WEN, C., PAN, W. and HUANG, M. (2017). Sure Independence Screening Adjusted for Confounding Covariates with Ultrahigh-dimensional Data. *Statistica Sinica* **28**. <https://doi.org/10.5705/ss.202014.0117>
- WANG, X., ZHU, J., PAN, W., ZHU, J. and ZHANG, H. (2021). Nonparametric statistical inference via metric distribution function in metric spaces. *arXiv preprint arXiv:2107.07317*.
- WEN, C., PAN, W., HUANG, M. and WANG, X. (2018). Sure independence screening adjusted for confounding covariates with ultrahigh dimensional data. *Statistica Sinica* 293-317.

- XUE, J. and LIANG, F. (2017). A Robust Model-Free Feature Screening Method for Ultrahigh-Dimensional Data. *Journal of Computational and Graphical Statistics* **26** 803-813. PMID: 30532512. <https://doi.org/10.1080/10618600.2017.1328364>
- ZHANG, S., PAN, J. and ZHOU, Y. (2018). Robust conditional nonparametric independence screening for ultrahigh-dimensional data. *Statistics & Probability Letters* **143** 95–101.
- ZHENG, Q., HONG, H. G. and LI, Y. (2020). Building generalized linear models with ultrahigh dimensional features: A sequentially conditional approach. *Biometrics* **76** 47–60.
- ZHU, J., PAN, W., ZHENG, W. and WANG, X. (2021). Ball: An R Package for Detecting Distribution Difference and Association in Metric Spaces. *Journal of Statistical Software, Articles* **97** 1–31. <https://doi.org/10.18637/jss.v097.i06>